# Tetracene Crystals as Promising Anode Material for Alkali Metal Ion Batteries

Chepkasov, I.; Krasheninnikov, A.;

Originally published:

June 2023

**Carbon 213(2023), 118190**

DOI: https://doi.org/10.1016/j.carbon.2023.118190

# Graphical Abstract

**Tetracene Crystals as Promising Anode Material for Alkali Metal Ion Batteries**

Ilya V. Chepkasov, Arkady V. Krasheninnikov

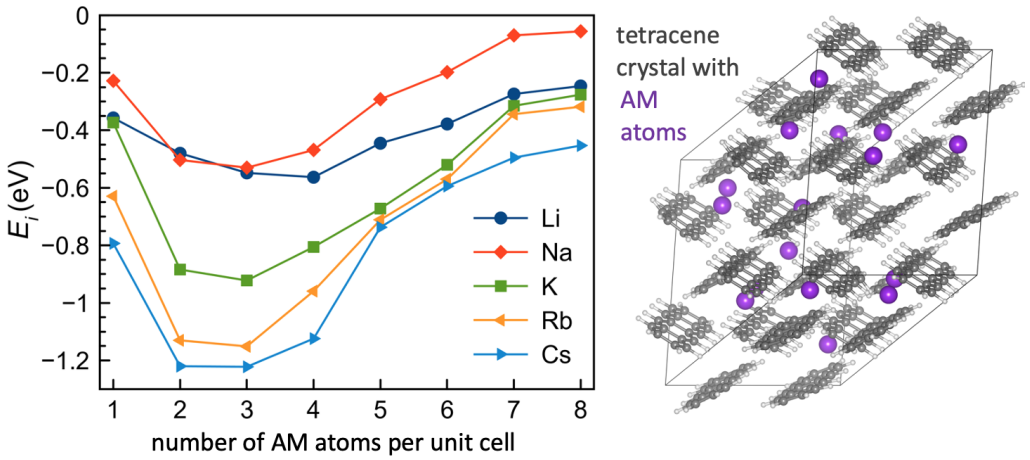

# Tetracene Crystals as Promising Anode Material for Alkali Metal Ion Batteries

Ilya V. Chepkasov[a], Arkady V. Krasheninnikov[a,b]

[a] *Helmholtz-Zentrum Dresden-Rossendorf, Institute of Ion Beam Physics and Materials Research, Dresden, D-01328, Germany*
[b] *Aalto University, Department of Applied Physics, FI-00076, Aalto, 11100, Finland*

**Abstract**

Using first-principles calculations we study the energetics of alkali metal (AM) atom intercalation into bulk tetracene crystals. We show that, contrary to the adsorption of Li and Na atoms on isolated tetracene molecules, the intercalation of these and other (K, Rb, Cs) AM atoms into bulk tetracene crystals is energetically favorable (with respect to forming an infinite AM crystal) in a wide range of AM concentrations and that the intercalation energy is noticeably lower than that for intercalation into graphite, a material used today in anodes of AM batteries. In case of Li, there is no swelling of the intercalated crystals, and for Na the increase in crystal volume is less than 10%, which makes crystalline tetracene attractive from the viewpoint of energy storage, as the capacity exceeds the theoretical capacity of graphite. We further assess diffusion barriers of AM atoms, which for Li and Na proved to be below 0.5 eV, indicating a high diffusivity of these atoms already at room temperature. We also study the effects of intercalation on the electronic properties of the system, and show that several bands can be filled upon intercalation, so that the system exhibits semiconducting-metallic-semiconducting behavior when AM atom concentration increases. Our results shed light on the perspective of using AM atom intercalation into tetracene crystals for energy storage and tuning the electronic properties of this system.

*Keywords:* tetracene, intercalation, alkali metal ions, first-principles calculations

*Email addresses:* ilyachepkasov@gmail.com (Ilya V. Chepkasov), a.krasheninnikov@hzdr.de (Arkady V. Krasheninnikov)

## 1. Introduction

The development of lightweight and compact but high-capacity rechargeable electrical power sources is crucial for further progress in ecologically-friendly technologies such as the manufacture and use of fully electric vehicles or renewable solar and wind energetics, which require large-scale energy storage facilities. Among them, Li-ion batteries (LIB)[1, 2, 3] are one of the most important sources due to their good efficiency and high energy density, as emphasized by the 2019 Nobel Prize in Chemistry, which was awarded for their development. Modern Li-ion batteries consist of the cathode and anode, and in order to meet the ever-increasing demand for high power and energy density, significant efforts have been made to search for high capacitance anode materials [2, 4, 5]. Among them, carbonaceous materials have attracted lots of attention because they can reversibly absorb and release Li-ions at a low electrochemical potential. Various types of carbon-containing materials have been considered as an anode, such as bulk graphite [6, 7], few-layer graphene [4, 5], and carbon nanotubes [8].

As Li reserves are limited, much research effort has also been focused on batteries with Na [9] and K [10] ions. However, due to the large size of Na and K atoms, traditional anode materials, e.g., graphite, which work well for Li, may not in general be suitable for Na and K atoms due to their low intercalation rate[10, 11] and undesirable volume changes upon intercalation/deintercalation, which has stimulated search for alternative systems.

In particular, polycyclic aromatic hydrocarbon (PAH) molecules, such as benzene, naphthalene, anthracene and tetracene have received lots of attention in that context [12, 13, 14]. PAH systems have been considered as prototypical carbonaceous materials, which mimic $sp^2$ allotropical forms of carbon, and also as organic solids capable of storing sufficiently high amount of energy to be of practical use. Specifically, Friedlein et al.[15] theoretically assessed the charge storage capability of PAH and showed that small and medium-size PAH might have the highest energy storage ability among all carbonaceous systems. Using density functional theory (DFT) calculations, Panigrahi and Sastry [16] studied the adsorption of Li atoms on a PAH molecules and demonstrated that the binding energy of Li atoms to PAH strongly depends on the position of the Li atom and the size of PAH. Porous tetracene-based materials have also theoretically been considered for Na and K storage [17].

Intercalation of alkali metal (AM) atoms into PAH crystals has also been

investigated [18] in the context of its electronic structure modification, e.g., to make the system superconducting [19]. K-intercalated PAH crystals were manufactured [20] and their structural and electro-magnetic properties were studied by a combination of spectroscopic techniques and DFT calculations. The crystal structure of K intercalated tetracene crystals and their electronic properties were aslo experimentally studied for various concentrations (up to two K per molecule) [21].

However, in spite of the prospects of PAH as anode materials, the intercalation of AM atoms into PAH crystals has not yet been studied in detail in the context of energy storage. Here we report the results of first-principles calculations of the intercalation of AMs in tetracene as the typical PAH system. We study the interaction of AMs with tetracene by considering both isolated molecules and bulk crystals, and also investigate the changes in the electronic characteristics of the system with increasing AM atom concentration.

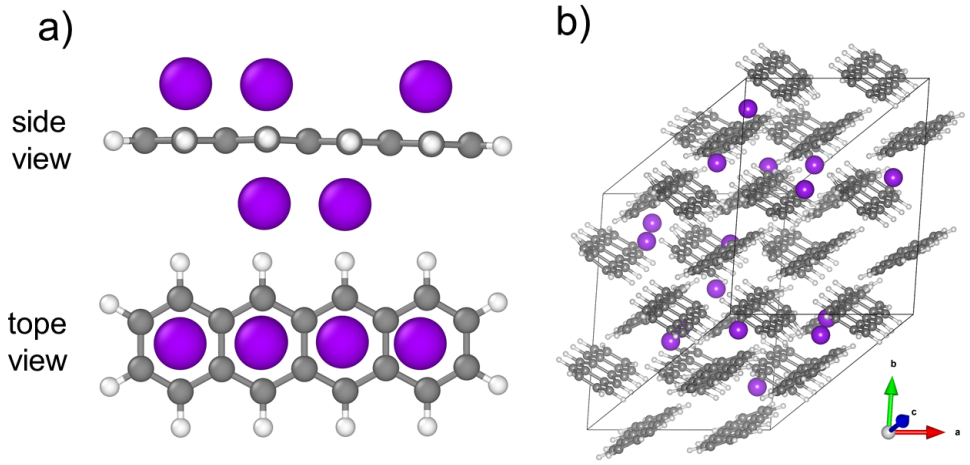


Figure 1: (a) Isolated tetracene molecule with adsorbed alkali metal (AM) atoms. (b) Thetracene crystal represented by a $2 \times 2 \times 2$ supercell with intercalated AM atoms. Large purple balls represent AM atoms, grey and white balls carbon and hydrogen atoms, respectively

## 2. Calculation methodology

All our calculations were carried out using the VASP software package [22, 23]. An energy cut-off of 600 eV was used for the supercells calculations. The Brillouin zones of the primitive cells of tetracene and alkali metals were sampled using $4\times4\times4$ and $12\times12\times12$ Monkhorst–Pack grid points [24]. The maximum force on each atom was set to be less than 0.01 eV for the optimized configurations. Our convergence tests indicated that the parameters we used were sufficient to assess the energetics with an accuracy of at least 0.02 eV. The atomic structures and the charge densities were illustrated using the VESTA package [25].

In this study we focused on tetracene, the typical PAH system. The unit cell of tetracene contains two molecules, which are arranged in herringbone layers in the *ab*-plane and stacked along the *c*-axis[26]. The $1 \times 1 \times 1$ and $2 \times 2 \times 2$ tetracene supercells containing 60 and 480 atoms were used in the calculations.

As van der Waals (vdW) forces contribute to the interaction of AM atoms with PAH molecules [27], the proper account for them is important. The vdW interaction can be modelled at different levels of sophistication, ranging from pair-wise interaction up to fully quantum-mechanical treatment, which is associated with lower/higher accuracy and the associated computational costs, see, e.g., [28, 29]. for an overview. In order to find a compromise between the accuracy and efficiency, we considered several vdW schemes (see Table S1). DFT-TS[30] and DFT-TS/HI[31] yield the lattice parameter of tetracene crystals which are in a good agreement with the experimental data, but these methods do not work well for alkali metals as shown previously [32]. The most accurate methods like vdW-DF [33] and optPBE-vdW [34] also give correct values of tetracene lattice parameters, but as showed we previously study [35] underestimate energy of bulk AMs, which affects the energetics of intercalation. At the same time, the computationally efficient zero damping DFT-D3 method [36] gives reasonable values of the lattice parameters and the energy, so that we used it in this study.

To assess the energetics directly related to the intercalation and relative stability of different configurations, we calculated the intercalation energy per AM atom, $E_i$, which corresponds to the energy change when $n_{AM}$ AM atoms are moved from the corresponding bulk AM crystal into the heterostructure, which is defined as

$$E_i = [E(n_{AM}) - E(0)]/n_{AM} - \mu_{AM}, \quad (1)$$

where $E(n_{AM})$ is the total energy of AM-intercalated tetracene system, $E(0)$ is energy of the pristine tetracene structure, and $\mu_{AM}$ - is the chemical potential of AM atom in the bulk structure (HCP in this study). Negative values indicate that it is energetically favorable for AM atoms to be intercalated, as compared to being in an infinite AM crystal.

In order to better understand the structural transformation which occur in the host upon intercalation, we also calculated the deformation energy $E_d$ which is defined as

$$E_d = E^* - E_0, \tag{2}$$

where $E^*$ is the energy of an isolated tetracene molecule with the geometry being the same as with the intercalant (the AM atoms are removed and the energy is calculated without geometry optimization) and $E_0$ is energy of the fully relaxed molecule.

Using the CI-NEB [37] approach, we assessed diffusion barriers for Li, Na, K, Rb and Cs atoms in tetracene crystals. Diffusion path consisted of 7 images. Diffusion barrier was calculated in the $2 \times 2 \times 2$ tetracene supercells.

## 3. Results and discussion

Prior to studying the intercalation of AM atoms (Li, Na, K, Rb, Cs) into bulk tetracene crystals, we considered the interaction of AM atoms with isolated molecules, and studied the absorption of AM atoms on an isolated tetracene molecule, Fig. 1(a). The number of adsorbed AM atoms varied from one to five. There are various possibilities for the adsorption of AM atoms on the tetracene molecule (next to each other, or with maximum separation, on the same or different sides of the molecule, etc.), and even for a single atom there are several inequivalent adsorption positions. All possible adsorption configurations we considered are shown in Fig. S1. In case of single AM atom there are two possibilities to interact with the molecule, that is to be adsorbed on the the terminal hexagonal ring (configuration $1a_1$) or in the middle of the molecule ($1a_2$). Our calculations showed that for Li, Na, K, Rb and Cs, single atom adsorption is preferable at the non-terminal hexagonal rings ($1a_2$). The difference between $E_i$ for the $1a_1$ and $1a_2$ positions, which is in this case the adsorption energy calculated using the energy of the bulk AM crystal as a references through equation 1, is 0.04 eV, 0.10 eV, 0.10 eV, 0.18 eV, 0.10 eV per AM atom for Li, Na, K, Rb and Cs respectively. In case of two AM atoms, the $2a_6$ configuration

was found to be preferable for Li, K, Rb, Cs, and $2a_5$ configuration for Na. Adsorption of more than two AM atoms on single molecule is energetically less favorable due to repulsive interaction between positively charged AM atoms, as shown earlier[16]. Overall, it is evident that AM atoms prefer to be spatially separated, ideally adsorbed on different molecules in the crystal.

To visualize the dependence of $E_i$ on the number of the adsorbed AM atoms $n_{AM}$, in Fig. 2 we plotted $E_i$ for the lowest energy configuration as a function of $n_{AM}$ for Li, Na, K, Rb, and Cs. With decreasing electronegativity from Na to Cs[38] $E_i$ decreases, which can be understood in terms of a stronger bonding due to a larger charge transfer, but in case of Li (except for a energetically unfavorable large number of adsorbed atoms) the trend is broken. Such a behavior for AM atoms intercalated into a bilayer graphene and graphite has been discussed earlier [39, 40, 41]. This effect is due to a strong covalent bonding between Li and carbon atoms [42] and the ionic contribution to the bonding. To illustrate this point, the charge difference between electron densities of the combined and separated system was visualized in Fig. 3. It is evident that the localization of charge in the covalent bonds between Li atoms and tetracene molecules is stronger (higher electron density concentration) than for other AM atoms.

The calculation of the electron transfer using the Bader charge analysis method [43] showed that a single AM atom on an isolated tetracene molecule loses approximately 0.87–0.86 electrons. With an increase in the number of atoms, the number of electrons per AM atom transferred to tetracene molecule decreases. An exception is the case with five Li atoms (position $5a_6$) where there is a significant deformation of the tetracene molecule, which leads to a change in the electronic properties and, as a result, a greater charge transfer to the molecule. To estimate the deformation of the tetracene molecule with adsorbed Li, Na, K, Rb and Cs atoms deformation energy ($E_d$) was calculated (Eq. 2). The value of the deformation energy is presented in Tables S2-S4. In the case of Li, the maximum deformation energy and an increase in charge transfer are observed for $5a_6$, configuration.

Having studied the interaction of AM atoms with isolated tetracene molecules, we simulated the AM atom intercalation into bulk tetracene crystals. AM atoms were added to the supercell, Fig. 1(b), and the structure was fully optimized. The concentration $x$ of AM atoms defined as the number of AM atoms per unit cell of tetracene was increased from zero up to eight. We note that two stable positions of a single AM atom in the supercell are possible, as illustrated in Fig. S3, and there are many configurations with roughly the

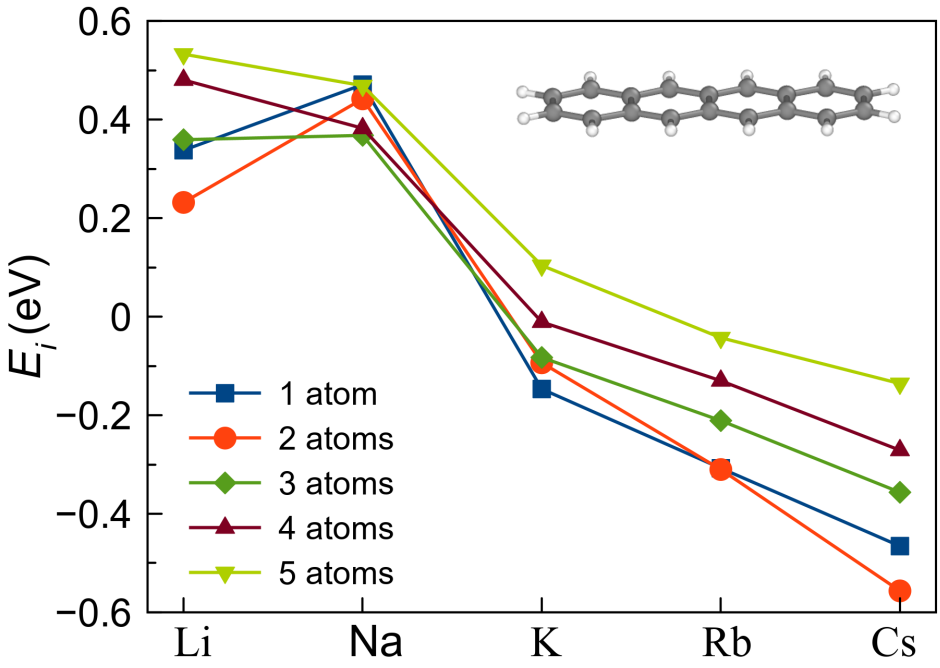


Figure 2: Energy required to take an AM atom from the bulk crystal and adsorb it on a free-standing tetracene molecule.

same energy when there are more than one AM atom in the supercell.

The intercalation energy $E_i$ calculated through Eq. 1 is presented in Fig. 4(a). It is evident that the values of $E_i$ are negative, which means that the intercalation is energetically favorable, even for Na, contrary to the intercalation into graphite [40] assuming that the 'conventional' $C_6LiC_6$ single- (not multi-layer [41]) structure with Li arranged in a commensurate $(\sqrt{3} \times \sqrt{3})R30°$ superstructure [44, 45, 40] is formed between graphene sheets. The minima observed at $x \sim 3$ ($x$=number of AM atoms/unit cell of tetracene) for all AM atoms indicate that spatially non-uniform intercalated crystals should be expected. The minima (for Li $x$=4, two Li atoms per tetracene molecule) is due to the fact that at high concentrations positively charged AM atoms begin to interact with each other.

The calculation of the charge transfer by the Bader method[43], Fig. 4(b), indicates that with increasing concentration of Li the number of electrons that each atom donates to the tetracene crystal is approximately 0.85-0.86

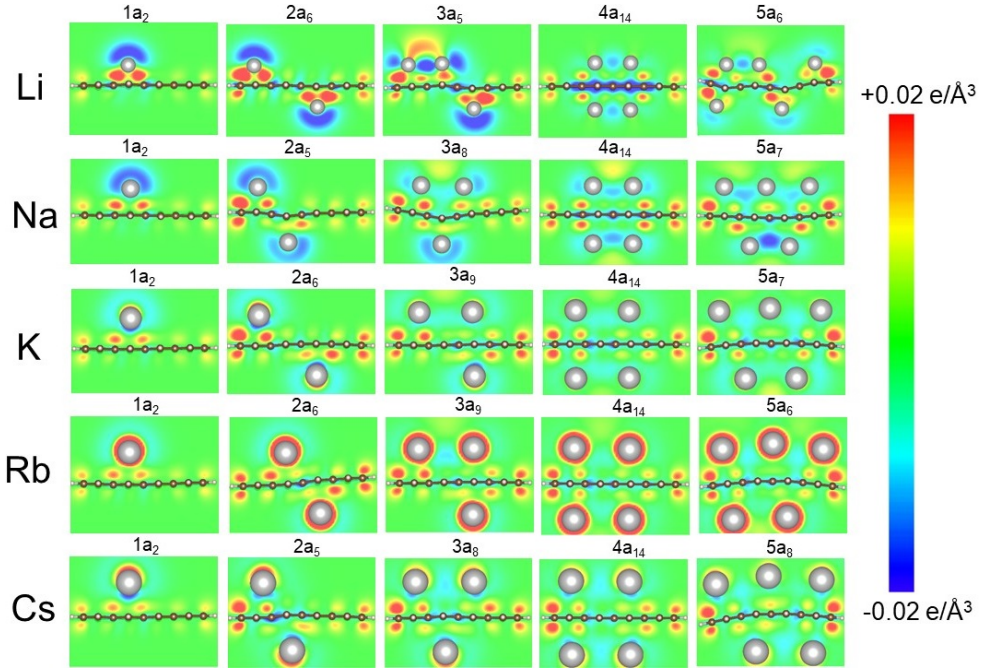


Figure 3: Charge transfer upon AM atom adsorption on a tetracene molecule, visualized as a difference between the electron density of a tetracene molecule with adsorbed AM atoms and the isolated molecule and the atoms. The charge difference is presented for the cross-section through the plane passing through the AM atoms and being perpendicular to the tetracene molecule plane. Note a build-up of the electron density between Li atoms and tetracene, indicative of covalent bonding. Red areas correspond to density build-up, blue to depletion.

$e^-$, and it is almost constant. In the case of Na, K and Rb, when their concentration increases, the number of electrons they donate to the tetracene crystal slightly decreases from 0.86-0.83$e^-$ to 0.80-0.79$e^-$. For Cs the changes in the number of electrons are larger, from 0.86 $e^-$ to 0.7$e^-$, which is associated with a larger change of the volume of the tetracene crystal upon intercalation, Fig. 4(c). Overall, the differences in the behavior of the transferred charge for Li and other alkali metal is related to the volume changes and the degree of covalent/ionic bonding between the intercalant and the host, as illustrated in Fig. 3. We note that the relatively small increase in the volume for Li and Na is an importnat result, hinting at the possibility of using tetracene crystals in the batteries.

To make the trends in the intercalation energy during intercalation of AM to tetracene crystal more evident, in Fig. 4(d) we plotted the changes in the

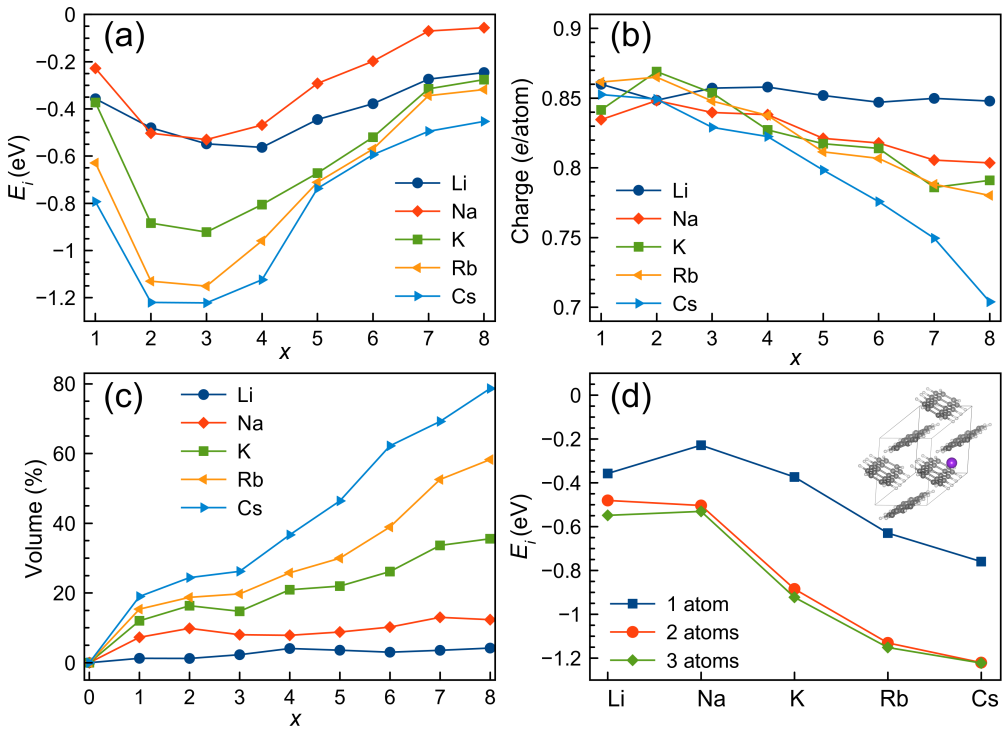


Figure 4: (a) Intercalation energy as a function of AM atom concentration $x$ (b) Charge transfer from AM atoms to tetracene crystal as a function of concentration of $x$, (c) Change of the volume of tetracene crystal vs. $x$. (d) Intercalation energy for AM atoms when one, two and three atoms per primitive cell are intercalated $x = 1, 2, 3$.

intercalation energy for a different number of AMs atoms. As in the case of the tetracene molecule, with decreasing electronegativity from Na to Cs, the energy is lowered, but in case of Li, the trend is reversed due to the covalent interaction between Li atoms and the molecules, as discussed previously.

We also calculated the capacity of the tetracene crystal (Fig. 5) with various concentrations of AM atoms. Theoretical capacity was calculated using Faraday's law. At a concentration of AM atoms more than $x$=6, the capacity of tetracene exceeds the theoretical capacity of graphite, which is widely used in ion batteries. In the case of Li and Na this concentrations are possible without a significant increase in the volume of tetracene. Thus hypothetically tetracene may be a more capacious anode material for Li-ion and Na-ion batteries than graphite.

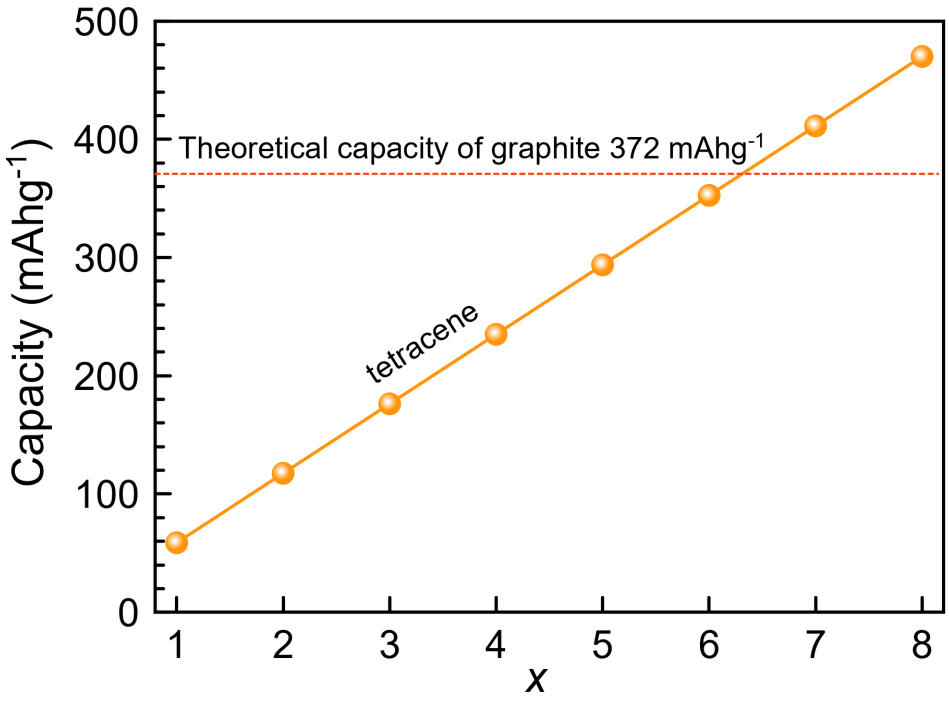


Figure 5: Capacity of the tetracene crystal with different concentrations of AM atoms.

For a deeper understanding of the intercalation processes at low concentrations of AM atoms, we also simulated the itercalation of Li, Na, K into a larger tetracene crystal represented by a $2 \times 2 \times 2$ supercell. The results are presented in Fig. S2(a). The oscillations in the dependence of the intercalation energy are due to the fact that the intercalated atoms were randomly intercalated in the supercell and did not necessarily occupy the most energetically favorable positions, which would have required extremely large amount of CPU time due to a large number of atoms in the system. Similar to the intercalation into $1 \times 1 \times 1$ supercell, with increase in the concentration, the amount of charge transferred decreases in case of K and Na, but remains unchanged for Li, about $0.86e^{-}$, Fig. S2(b).

To get insight into the intercalation kinetics, we also assessed the diffusion barriers for the intercalated atoms. The intercalant atom diffusivity is an important factor, which may govern the actual operation of the ion battery, as the charge/discharge of metal-ion batteries mainly depends on the diffusion of AM atoms in the anode materials. Using the CI-NEB [37]

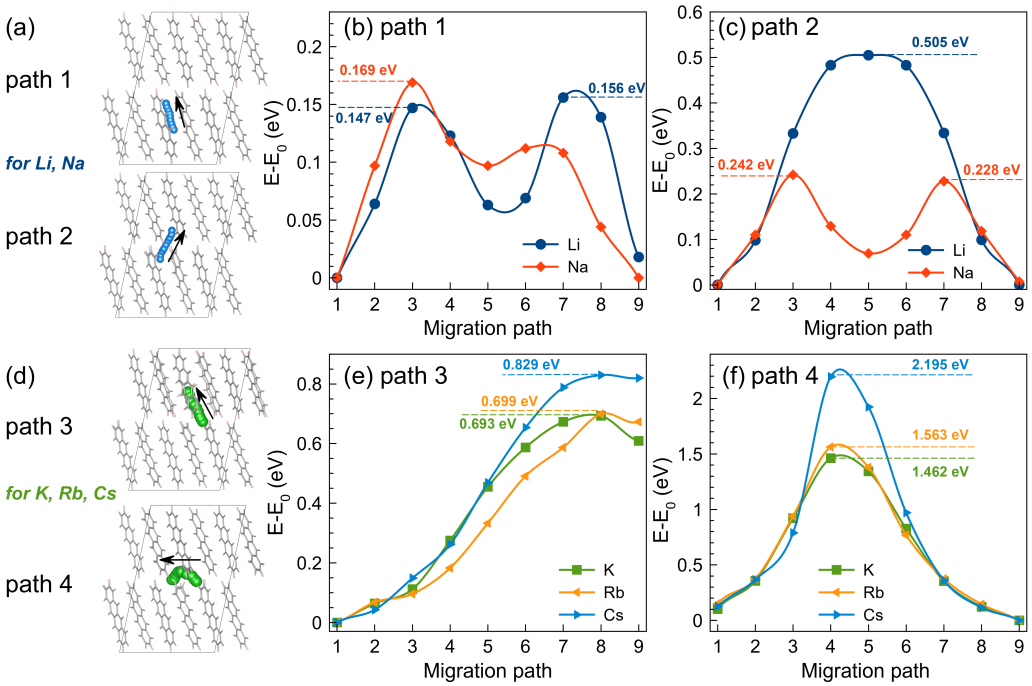


Figure 6: (a) Diffusion paths for Li and Na atoms between and along the molecules in a tetracene crystal. (b) Migration barrier of Li and Na along the tetracene molecule. (c) The barrier of Li and Na for migration from one molecule to another. (d) Diffusion paths for K, Rb, Cs along the molecules and along the stacks of tetracene molecules in a tetracene crystal. (e) Migration barrier for K, Rb, Cs along the tetracene molecule. (f) Migration barrier for K, Rb, Cs along the stacks of tetracene molecules.

approach we calculated diffusion barriers for Li, Na, K, Rb and Cs atoms. It was determined that for different types of alkali metal atoms different positions in the tetracene crystal are most energetically favorable, Fig. S3(a). For example, for Li and Na atoms, the most favorable position is between tetracene molecules (position 1 in Fig. S3(b)). It is interesting that in case of Na, the difference in energy between position 1 and position 2 is rather small, that can be key for understanding the low Na barrier. On the other hand for K, Rb and Cs atoms, it is more energetically favorable to be between the stacked tetracene molecules (position 2 in Fig. S3(b)). For this reason, different diffusion paths were chosen for Li, Na (path1, path2) and for K, Rb, Cs (path3, path4). The diffusion paths are presented in Fig. 6(a) for Li, Na and in Fig. 6(d) for K, Rb, Cs. The associated energy barriers are shown in Fig. 6(b,c,e,f). It is evident that the barriers for Li and Na are

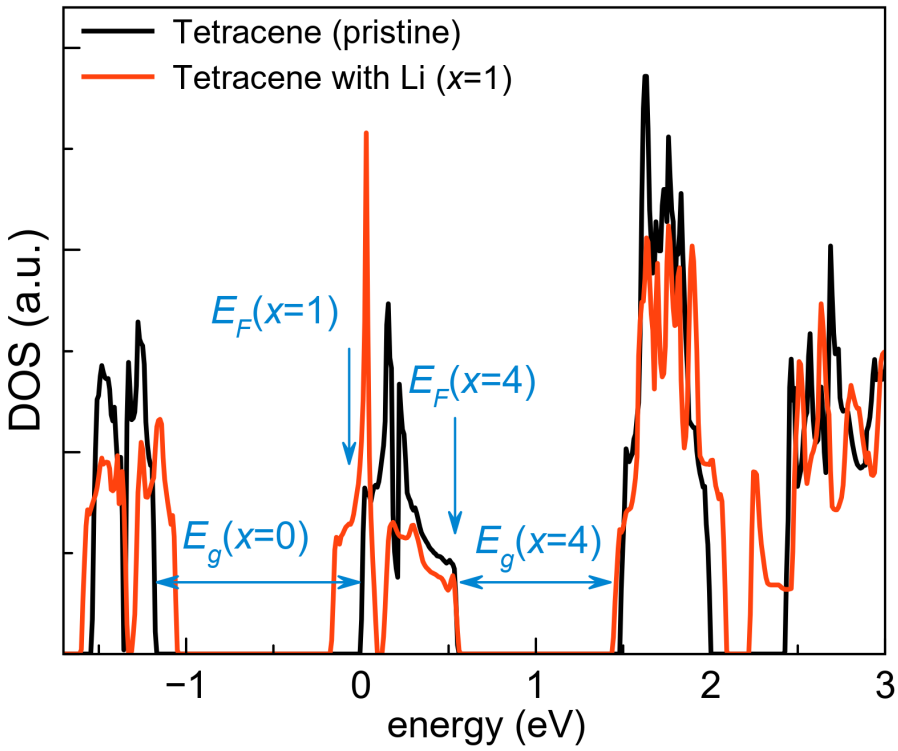


Figure 7: Density of states of pristine tetracene crystal and with Li ($x$=1). Zero energy corresponds to conduction band minimum in the absence of doping.

relatively low, so that the diffusion should be possible at room temperature, but the diffusion is governed by the 'jumps' between the molecules. With regard to the diffusion along the molecule, the obtained values for Li are in good agreement with the values of the diffusion in BLG (AA stacking energy barrier 0.34 eV, for AB stacking 0.07 eV) [46]. The diffusion barrier for Na is slightly lower than for Li, which is consistent with previous calculations of the diffusion of Li and Na for example in case of graphene [47]. The diffusion barrier for K, Rb and Cs are quite high.

Finally, keeping in mind the possibility to tune the electronic structure of tetracene crystals, we investigated the effects of intercalation on their electronic properties. Previous DFT studies of the electronic properties of tetracene showed that the system is a semiconductor with a band gap of 1.23 eV[48]. Our calculations gave a close value of 1.17 eV. The densities of

states (DOS) of the pristine and intercalated systems are shown in Fig. 7. The calculations of the electronic structure of the tetracene crystals indicate that the intercalation by Li, Na, K, Rb, and Cs atoms (low concentration of the AM atoms) gives rise to the shift of the Fermi energy to the conduction band minimum, so that the system becomes metallic, as illustrated in Fig. 7(b). Increase of the AM atom concentration $x$ gives rise to the full filling of the first empty band, and a new gap separates filled and empty states. The value of the gap varies for different AM, as the DOS slightly changes. At a concentration $x$=4 in cases of Li, Na, K, Rb and Cs the band gap is 1.07 eV, 1.1 eV, 1.2 eV, 0.76 eV and 1.03 eV respectively.

## 4. Conclusions

In summary, by employing DFT calculations we investigated the adsorption of alkali metal (AM) atoms on isolated tetracene molecules, the typical polycyclic aromatic hydrocarbons, and their intercalation into bulk tetracene crystals. We showed that, while adsorption of Li and Na atoms on isolated tetracene molecules is energetically unfavorable with respect to being in an infinite AM crystal, the intercalation of these and other (K, Rb, Cs) AM atoms into bulk tertacene crystals is associate with energy release in a wide range of AM concentrations. Moreover, the intercalation energy is noticeably lower than that for intercalation into graphite, a material used today in anodes of AM batteries. In case of Li, there is no swelling of the intercalated crystals, and for Na the increase in crystal volume is less than 10%, which makes crystalline tetracene attractive from the viewpoint of energy storage, as the capacity exceeds the theoretical capacity of graphite. We also calculated diffusion barriers for all AM atoms we considered. For Li and Na atoms along and between the molecules, the barriers proved to be below 0.5 eV, indicating a high diffusivity of these AM atoms already at room temperature. The diffusion barrier for K, Rb and Cs proved to be rather high, indicating that diffusion of these AM atoms at room temperature is slow. We further studied the effects of intercalation on the electronic properties of tetracene crystals, and demonstrated that depending on AM atom concentration, several bands can be filled upon intercalation, so that the system exhibits first metallic then again semiconducting behavior. Overall, our results provide insights into the energetics and kinetics of AM atom intercalation into tetracene crystals in the context of energy storage and tuning the electronic properties of this system.

## Declaration of competing interest

The authors declare that they have no known competing financial interests or personal relationships that could have appeared to influence the work reported in this paper.

## Acknowledgement

A.V.K. acknowledges the German Research Foundation (DFG) for the support through Project KR 4866/9-1 and the collaborative research center "Chemistry of Synthetic 2D Materials" SFB-1415-417590517. I.V.C. thanks the German Academic Exchange Service (DAAD) program "Mikhail Lomonosov" for support. The authors thank the HZDR Computing Center, HLRS, Stuttgart, Germany, and TU Dresden Cluster "Taurus" for generous grants of CPU time. We would also like to thank Jens Pflaum and Maximillian Frank for discussions and for attracting our attention to the problem of alkali metal atom intercalation into organic molecular crystals.

## References

[1] J. Xie, Y.-C. Lu, A retrospective on lithium-ion batteries, Nature Communications 11 (1) (2020) 2499. doi:10.1038/s41467-020-16259-9.

[2] J. Xu, Y. Dou, Z. Wei, J. Ma, Y. Deng, Y. Li, H. Liu, S. Dou, Recent progress in graphite intercalation compounds for rechargeable metal (li, na, k, al)-ion batteries, Advanced Science 4 (10) (2017) 1700146. doi:10.1002/advs.201700146.

[3] J. Janek, W. G. Zeier, A solid future for battery development, Nature Energy 1 (9) (2016) 16141. doi:10.1038/nenergy.2016.141.

[4] K. Ji, J. Han, A. Hirata, T. Fujita, Y. Shen, S. Ning, P. Liu, H. Kashani, Y. Tian, Y. Ito, J.-i. Fujita, Y. Oyama, Lithium intercalation into bilayer graphene, Nature Communications 10 (1) (2019) 275. doi:10.1038/s41467-018-07942-z.

[5] F. J. Sonia, M. K. Jangid, B. Ananthoju, M. Aslam, P. Johari, A. Mukhopadhyay, Understanding the li-storage in few layers graphene with respect to bulk graphite: experimental, analytical and computational study, Journal of Materials Chemistry A 5 (18) (2017) 8662–8679. doi:10.1039/C7TA01978E.

[6] H. Zhang, Y. Yang, D. Ren, L. Wang, X. He, Graphite as anode materials: Fundamental mechanism, recent progress and advances, Energy Storage Materials 36 (2021) 147–170. doi:10.1016/j.ensm.2020.12.027.

[7] J. Asenbauer, T. Eisenmann, M. Kuenzel, A. Kazzazi, Z. Chen, D. Bresser, The success story of graphite as a lithium-ion anode material–fundamentals, remaining challenges, and recent developments including silicon (oxide) composites, Sustainable Energy & Fuels 4 (11) (2020) 5387–5416. doi:10.1039/D0SE00175A.

[8] H. Shimoda, B. Gao, X. P. Tang, A. Kleinhammes, L. Fleming, Y. Wu, O. Zhou, Lithium intercalation into opened single-wall carbon nanotubes: Storage capacity and electronic properties, Phys. Rev. Lett. 88 (2001) 015502. doi:10.1103/PhysRevLett.88.015502.

[9] Y.-S. Hu, Y. Li, Unlocking sustainable na-ion batteries into industry, ACS Energy Letters 6 (11) (2021) 4115–4117. doi:10.1021/acsenergylett.1c02292.

[10] A. K. Thakur, M. S. Ahmed, J. Park, R. Prabakaran, S. Sidney, R. Sathyamurthy, S. C. Kim, S. Periasamy, J. Kim, J.-Y. Hwang, A review on carbon nanomaterials for k-ion battery anode: Progress and perspectives, International Journal of Energy Research (2021). doi:doi.org/10.1002/er.7508.

[11] E. Olsson, J. Yu, H. Zhang, H.-M. Cheng, Q. Cai, Atomic-scale design of anode materials for alkali metal (li/na/k)-ion batteries: Progress and perspectives, Advanced Energy Materials 12 (25) (2022) 2200662. doi:10.1002/aenm.202200662.

[12] D. Kong, T. Cai, H. Fan, H. Hu, X. Wang, Y. Cui, D. Wang, Y. Wang, H. Hu, M. Wu, et al., Polycyclic aromatic hydrocarbons as a new class of promising cathode materials for aluminum-ion batteries, Angewandte Chemie International Edition 61 (3) (2022) e202114681. doi:10.1002/anie.202114681.

[13] J. H. Park, T. Liu, K. C. Kim, S. W. Lee, S. S. Jang, Systematic molecular design of ketone derivatives of aromatic molecules for lithium-ion batteries: First-principles dft modeling, ChemSusChem 10 (7) (2017) 1584–1591. doi:10.1002/cssc.201601730.

[14] P. K. Ramya, C. H. Suresh, Polycyclic aromatic hydrocarbons as anode materials in lithium-ion batteries: A dft study, The Journal of Physical Chemistry A 127 (11) (2023) 2511–2522. doi:10.1021/acs.jpca.3c00337.

[15] R. Friedlein, X. Crispin, W. R. Salaneck, Molecular parameters controlling the energy storage capability of lithium polyaromatic hydrocarbon intercalation compounds, Journal of Power Sources 129 (1) (2004) 29–33. doi:10.1016/j.jpowsour.2003.11.018.

[16] S. Panigrahi, G. N. Sastry, Reducing polyaromatic hydrocarbons: the capability and capacity of lithium, RSC Advances 4 (28) (2014) 14557–14563. doi:doi.org/10.1039/C3RA47326K.

[17] U. Younis, I. Muhammad, Y. Kawazoe, Q. Sun, Design of tetracene-based metallic 2d carbon materials for na-and k-ion batteries, Applied Surface Science 521 (2020) 146456. doi:10.1016/j.apsusc.2020.146456.

[18] F. D. Romero, M. Pitcher, C. Hiley, G. Whitehead, S. Kar, A. Ganin, D. Antypov, C. Collins, M. Dyer, G. Klupp, et al., Redox-controlled potassium intercalation into two polyaromatic hydrocarbon solids, Nature Chemistry 9 (7) (2017) 644–652. doi:10.1038/nchem.2765.

[19] R. Mitsuhashi, Y. Suzuki, Y. Yamanari, H. Mitamura, T. Kambe, N. Ikeda, H. Okamoto, A. Fujiwara, M. Yamaji, N. Kawasaki, et al., Superconductivity in alkali-metal-doped picene, Nature 464 (7285) (2010) 76–79. doi:10.1038/nature08859.

[20] Q. T. Phan, S. Heguri, H. Tamura, T. Nakano, Y. Nozue, K. Tanigaki, Two different ground states in k-intercalated polyacenes, Physical Review B 93 (7) (2016) 075130. doi:10.1103/PhysRevB.93.075130.

[21] C. I. Hiley, K. K. Inglis, M. Zanella, J. Zhang, T. D. Manning, M. S. Dyer, T. Knaflic, D. Arcon, F. Blanc, K. Prassides, et al., Crystal structure and stoichiometric composition of potassium-intercalated tetracene, Inorganic Chemistry 59 (17) (2020) 12545–12551. doi:10.1021/acs.inorgchem.0c01635.

[22] G. Kresse, J. Furthmüller, Efficient iterative schemes for ab initio total-energy calculations using a plane-wave basis set, Physical Review B 54 (16) (1996) 11169. doi:10.1103/PhysRevB.54.11169.

[23] G. Kresse, D. Joubert, From ultrasoft pseudopotentials to the projector augmented-wave method, Physical Review B 59 (3) (1999) 1758. doi:10.1103/PhysRevB.59.1758.

[24] H. J. Monkhorst, J. D. Pack, Special points for brillouin-zone integrations, Physical Review B 13 (12) (1976) 5188. doi:10.1103/PhysRevB.13.5188.

[25] K. Momma, F. Izumi, Vesta: a three-dimensional visualization system for electronic and structural analysis, Journal of Applied Crystallography 41 (3) (2008) 653–658. doi:10.1107/S0021889808012016.

[26] D. Holmes, S. Kumaraswamy, A. J. Matzger, K. P. C. Vollhardt, On the nature of nonplanarity in the [n] phenylenes, Chemistry–A European Journal 5 (11) (1999) 3399–3412. doi:10.1002/(SICI)1521-3765(19991105)5:11¡3399::AID-CHEM3399¿3.0.CO;2-V.

[27] B. Schatschneider, S. Monaco, A. Tkatchenko, J.-J. Liang, Understanding the structure and electronic properties of molecular crystals under pressure: application of dispersion corrected dft to oligoacenes, The Journal of Physical Chemistry A 117 (34) (2013) 8323–8331. doi:10.1021/jp406573n.

[28] S. A. Tawfik, T. Gould, C. Stampfl, M. J. Ford, Evaluation of van der waals density functionals for layered materials, Physical Review Materials 2 (3) (2018) 034005. doi:10.1103/PhysRevMaterials.2.034005.

[29] A. Tkatchenko, Current Understanding of Van der Waals Effects in Realistic Materials, Advanced Functional Materials 25 (13) (2015) 2054–2061. doi:10.1002/adfm.201403029.

[30] A. Tkatchenko, M. Scheffler, Accurate molecular van der waals interactions from ground-state electron density and free-atom reference data, Physical Review Letters 102 (7) (2009) 073005. doi:10.1103/PhysRevLett.102.073005.

[31] T. Bucko, S. Lebegue, J. Hafner, J. G. Angyan, Improved density dependent correction for the description of london dispersion forces, Journal of Chemical Theory and Computation 9 (10) (2013) 4293–4299. doi:10.1021/ct400694h.

[32] J. Park, B. D. Yu, S. Hong, Van der waals density functional theory study for bulk solids with bcc, fcc, and diamond structures, Current Applied Physics 15 (8) (2015) 885–891. doi:10.1016/j.cap.2015.03.028.

[33] M. Dion, H. Rydberg, E. Schröder, D. C. Langreth, B. I. Lundqvist, Van der waals density functional for general geometries, Physical Review Letters 92 (24) (2004) 246401. doi:10.1103/PhysRevLett.92.246401.

[34] J. Klimeš, D. R. Bowler, A. Michaelides, Chemical accuracy for the van der waals density functional, Journal of Physics: Condensed Matter 22 (2) (2009) 022201. doi:10.1088/0953-8984/22/2/022201.

[35] I. V. Chepkasov, J. H. Smet, A. V. Krasheninnikov, Single-and multi-layers of alkali metal atoms inside graphene/mos2 heterostructures: A systematic first-principles study, The Journal of Physical Chemistry C 126 (37) (2022) 15558–15564. doi:10.1021/acs.jpcc.2c03749.

[36] S. Grimme, J. Antony, S. Ehrlich, H. Krieg, A consistent and accurate ab initio parametrization of density functional dispersion correction (dft-d) for the 94 elements h-pu, The Journal of Chemical Physics 132 (15) (2010) 154104. doi:10.1063/1.3382344.

[37] G. Henkelman, B. P. Uberuaga, H. Jónsson, A climbing image nudged elastic band method for finding saddle points and minimum energy paths, The Journal of Chemical Physics 113 (22) (2000) 9901–9904. doi:10.1063/1.1329672.

[38] C. Tantardini, A. R. Oganov, Thermochemical electronegativities of the elements, Nature Communications 12 (1) (2021) 2087. doi:10.1038/s41467-021-22429-0.

[39] Y. Liu, B. V. Merinov, W. A. Goddard, Origin of low sodium capacity in graphite and generally weak substrate binding of na and mg among alkali and alkaline earth metals, Proceedings of the National Academy of Sciences 113 (14) (2016) 3735–3739. doi:10.1073/pnas.1602473113.

[40] H. Moriwake, A. Kuwabara, C. A. Fisher, Y. Ikuhara, Why is sodium-intercalated graphite unstable?, RSC Advances 7 (58) (2017) 36550–36554. doi:10.1039/C7RA06777A.

[41] I. V. Chepkasov, M. Ghorbani-Asl, Z. I. Popov, J. H. Smet, A. V. Krasheninnikov, Alkali metals inside bi-layer graphene and mos2: Insights from first-principles calculations, Nano Energy 75 (2020) 104927. doi:10.1016/j.nanoen.2020.104927.

[42] C. Hartwigsen, W. Witschel, E. Spohr, Charge density and charge transfer in stage-1 alkali-graphite intercalation compounds, Physical Review B 55 (8) (1997) 4953. doi:10.1103/PhysRevB.55.4953.

[43] W. Tang, E. Sanville, G. Henkelman, A grid-based bader analysis algorithm without lattice bias, Journal of Physics: Condensed Matter 21 (8) (2009) 084204. doi:10.1088/0953-8984/21/8/084204.

[44] S. Yang, S. Li, S. Tang, W. Dong, W. Sun, D. Shen, M. Wang, Sodium adsorption and intercalation in bilayer graphene from density functional theory calculations, Theoretical Chemistry Accounts 135 (7) (2016) 164. doi:10.1007/s00214-016-1910-0.

[45] Z. Wang, S. M. Selbach, T. Grande, Van der waals density functional study of the energetics of alkali metal intercalation in graphite, RSC Advances 4 (8) (2014) 4069–4079. doi:10.1039/C3RA47187J.

[46] K. Zhong, R. Hu, G. Xu, Y. Yang, J.-M. Zhang, Z. Huang, Adsorption and ultrafast diffusion of lithium in bilayer graphene: Ab initio and kinetic monte carlo simulation study, Physical Review B 99 (15) (2019) 155403. doi:10.1103/PhysRevB.99.155403.

[47] S. Mukherjee, L. Kavalsky, K. Chattopadhyay, C. V. Singh, Dramatic improvement in the performance of graphene as li/na battery anodes with suitable electrolytic solvents, Carbon 161 (2020) 570–576. doi:10.1016/j.carbon.2020.02.001.

[48] K. Hummer, C. Ambrosch-Draxl, Electronic properties of oligoacenes from first principles, Physical Review B 72 (20) (2005) 205205. doi:10.1103/PhysRevB.72.205205.